Published in final edited form as:
Protein J. 2014 June ; 33(3): 267–277. doi:10.1007/s10930-014-9559-9.

Electron Paramagnetic Resonance Spectroscopy of Nitroxide-Labeled Calmodulin

Paula B. Bowman[a,*] and **David Puett**[b,c,**]

[a]Department of Biochemistry, Vanderbilt University School of Medicine, Nashville, TN 37232

[b]Department of Biochemistry and Molecular Biology, University of Georgia, Athens, GA 30602

[c]Department of Biochemistry and Biophysics, University of North Carolina School of Medicine, Chapel Hill, NC 27599

Abstract

Calmodulin (CaM) is a highly conserved calcium-binding protein consisting of two homologous domains, each of which contains two EF-hands, that is known to bind well over 300 proteins and peptides. In most cases the $(Ca^{2+})_4$-form of CaM leads to the activation of a key regulatory enzyme or protein in a myriad of biological processes. Using the nitroxide spin-labeling reagent, 3-(2-iodoacetamido)-2,2,5,5-tetramethyl-1-pyrrolidinyl oxyl, bovine brain CaM was modified at 2-3 methionines with retention of activity as judged by the activation of cyclic nucleotide phosphodiesterase. X-band electron paramagnetic resonance (EPR) spectroscopy was used to measure the spectral changes upon addition of Ca^{2+} to the apo-form of spin-labeled protein. A significant loss of spectral intensity, arising primarily from reductions in the heights of the low, intermediate, and high field peaks, accompanied Ca^{2+} binding. The midpoint of the Ca^{2+}-mediated transition determined by EPR occurred at a higher Ca^{2+} concentration than that measured with circular dichroic spectroscopy and enzyme activation. Recent data have indicated that the transition from the apo-state of CaM to the fully saturated form, $[Ca^{2+})_4$-CaM], contains a compact intermediate corresponding to $[Ca^{2+})_2$-CaM], and the present results suggest that the spin probes are reporting on Ca^{2+} binding to the last two sites in the N-terminal domain, i.e. for the $[Ca^{2+})_2$-CaM] $\rightarrow$ $[Ca^{2+})_4$-CaM] transition in which the compact structure becomes more extended. EPR of CaM, spin-labeled at methionines, offers a different approach for studying Ca^{2+}-mediated conformational changes and may emerge as a useful technique for monitoring interactions with target proteins.

Keywords

Calmodulin; Calcium binding; Spin labeling; Nitroxide; Electron paramagnetic resonance; Circular dichroism; Phosphodiesterase

**To whom correspondence should be addressed. puett@bmb.uga.edu.
*Formerly Paula B. Hewgley.

Conflict of interest The authors declare no conflict of interest.

Ethical standards The experiments presented herein comply with the current laws of the USA.

1 Introduction

The Ca^{2+}-binding eukaryotic protein, calmodulin (CaM), has been well characterized with regard to structure and biological function [1, 2]. An abundant, relatively small (M_r ~ 17kDa), and highly conserved protein, CaM contains four EF-hands, each of which binds Ca^{2+} with μM affinity. The homologous N-terminal and C-terminal domains of the protein each contain two EF-hands, with the two in the C-terminal lobe having a slightly higher affinity for Ca^{2+} than those in the N-terminal lobe.

A number of structures of apo-CaM, $(Ca^{2+})_2$-CaM (in complex), $(Ca^{2+})_4$-CaM, and $(Ca^{2+})_4$-CaM-protein/peptide complexes are available from X-ray crystallography and NMR spectroscopy [3-11]. From these and many other reports [12] it is known that in the Ca^{2+}-free form, or apo-state, CaM has a rather compact structure that, concomitant with Ca^{2+} binding, opens to an extended `dumbbell-like` structure with a flexible eight-turn central α-helix and a change in the relative orientations of the helices surrounding each Ca^{2+} binding site. Accompanying this dramatic conformational change, two hydrophobic patches rich in methionine are formed. In this conformation, CaM can bind to and activate over 350 different proteins [cf. website maintained by the Ikura group, http://calcium.uhnres.utoronto.ca/ctdb/, and described in ref. 13], in many cases regulating key pathways in numerous biological processes. This promiscuity can be attributed to a combination of the flexible nature of the central helix [14] and the hydrophobic patches [15] that exist in $(Ca^{2+})_4$-CaM. A recent analysis of the CaM-protein/peptide complexes available in the Protein Data Bank (› 80 unique structures deposited) showed many diverse binding modalities, emphasizing the conformational flexibility of Ca^{2+}-activated CaM [16].

In addition to X-ray crystallography and NMR spectroscopy, numerous biophysical approaches have been used to study Ca^{2+}-mediated conformational changes in CaM, including circular dichroism (CD) [17, 18], fluorescence [19], infrared spectroscopy [20], Föster resonance energy transfer [21], hydrodynamics [22], and other techniques as well. Electron paramagnetic resonance (EPR), the focus of this study, has emerged as a highly specific, sensitive, and informative method to investigate proteins [23-32]. Several laboratories have reported on the use of EPR to monitor the binding of Ca^{2+}, other cations, and other molecules to CaM [33-45]. Others have used spin-labeled peptides of target proteins to study their interaction with CaM [46].

The objective of the present investigation was to compare the Ca^{2+} dependence of EPR spectral changes of spin-labeled CaM (SL-CaM) with the changes obtained by CD spectroscopy and cyclic nucleotide phosphodiesterase (PDE) activation. The nitroxide radical was used for spin labeling, in large part because of its stability in water and wide use with biological macromolecules [47-50]. It was found that the major changes in the EPR spectra occurred at a higher Ca^{2+} concentration than changes determined by CD and PDE activation, attributed to filling of the two Ca^{2+}-binding sites in the N-terminal portion of CaM. This CaM derivative may prove useful in probing the interactions of CaM with target proteins.

2 Experimental Procedures

2.1 Calmodulin Purification, Spin Labeling, and Chemical Characterization

CaM was purified to homogeneity from bovine brain using a combination of ammonium sulfate fractionation, ion-exchange chromatography, and gel exclusion chromatography, and then chemically modified as described elsewhere [33]. Nitroxide spin labeling of calmodulin methionyl residues was accomplished with 3-(2-iodoacetamido)-2,2,5,5-tetramethyl-1-pyrrolidinyl oxyl (purchased from Syva Corp., Palo Alto, CA), generally in a 20-fold excess of spin label to protein. The purified protein was dissolved in 0.1 M sodium succinate buffer, pH 5.8, containing 0.1 mM $CaCl_2$. The spin-labeling reagent, poorly soluble in water, was taken up in 0.1 mL ethanol and then added to 1 mL succinate buffer with sonication, yielding a finely divided suspension. Next, the suspension was added drop-wise to 5 mL of the protein solution with stirring. The mixing vial was wrapped in aluminum foil, flushed with nitrogen, and continually stirred for 24 h at 37°C. The solution was then exhaustively dialyzed against 0.1 M NH_4HCO_3 and lyophilized. A protein recovery of 65-85% was obtained. Stock solutions of SL-CaM were prepared in 50 mM Tris-HCl, pH 7.5, and 2 mM EGTA. To achieve various concentrations of free Ca^{2+}, $(Ca^{2+})_f$, the method given in the Supplement was employed. Briefly, a 2 mM EGTA/$CaCl_2$ system was used in 50 mM Tris-HCl to achieve the desired free Ca^{2+} concentration and maintain a constant pH. During the Ca^{2+} titrations, the concentration of SL-CaM decreased from 15.4 μM to 14.6 μM, and appropriate corrections were made to refer all values to the starting protein concentration. The native and spin labeled proteins were characterized chemically and physicochemically using a variety of techniques as described in the Supplement.

2.2 Phosphodiesterase Preparation and Assay

A PDE fraction was prepared from bovine brain using ammonium sulfate fractionation and ion-exchange chromatography on DEAE-Sephadex A-50 [33]. The CaM-dependent enzyme was assayed (30 min, 30°C) using 1 μM [^{3}H]cGMP in a 20 mM Tris-HCl, pH 7.5 buffer containing 2 mg/mL bovine serum albumin, and different concentrations of Ca^{2+}. The [^{3}H]5′-monophosphate was converted to [^{3}H]guanosine by snake venom nucleotidase and then separated from [^{3}H]cGMP by chromatography on QAE-Sephadex A-25 with 20 mM NH_4CHO_2, pH 7.4 and counted [33, 34] (see [51] for a recent review on phosphodiesterase assays). CaM and SL-CaM were each assayed at 3 μM, where enzyme activation was maximal.

2.3 CD Spectroscopy

CD spectra of CaM and SL-CaM were collected at ambient temperature in a 2 mm cell with a Cary 60 spectropolarimeter equipped with a CD attachment. The instrument was operated with a time constant of 3 sec and a full-scale deflection of 100 mdeg; duplicate or triplicate scans of baseline and samples were made and reproducibility was excellent. For example, at 222 nm the mean residue ellipticity varied by less than 500 deg·cm^2/dmol. The average was taken, and the mean residue ellipticity calculated in units of deg·cm^2/dmol. The spectra were taken in 50 mM Tris-HCl, pH 7.5, containing 2 mM EGTA with no added Ca^{2+} (0 mM Ca^{2+}) or EGTA:$CaCl_2$ ratios to yield a desired free Ca^{2+} concentration, i.e. the same as used

for EPR spectroscopy. Spectra of denatured CaM and SL-CaM were taken in 7 M guanidinium chloride containing 4 mM Tris-HCl, pH 7.5 and 20 mM EGTA.

2.4 X-band EPR Spectroscopy

A Varian E-112 spectrometer equipped with a TE_{102} microwave cavity (Varian E-231) was used to measure EPR spectra at ambient temperature. The following settings were used during measurements: 0.5 Gauss modulation amplitude, 5 milliwatts (mW) microwave power, X-band frequency (9.5 GHz), 100 kilohertz field modulation, 16 min time scans, 0.128 sec time constant, and 2.0×10^4 receiver gain. For power saturation studies, 100 Gauss scans on SL-CaM ± Ca^{2+} were also done at microwave powers between 1 - 150 mW. All EPR spectra were collected on SL-CaM solutions at various Ca^{2+} concentrations in standard flat cells with a buffer of 50 mM Tris-HCl, pH 7.5 containing 2 mM EGTA with no added Ca^{2+} (0 mM Ca^{2+}) or EGTA:$CaCl_2$ ratios to give a designated free Ca^{2+} concentration. For these Ca^{2+} titrations a total of 16 concentrations from 0 – 8.1 mM Ca^{2+} were used with duplicate scans for nine concentrations and 3 – 5 scans for seven concentrations. Each point shows the range or SEM, although in many cases the symbol size exceeded the range or SEM. EPR spectra of the free spin label were collected in the same buffer used for SL-CaM, but these were 40 Gauss scans determined in duplicate. Spectral intensities (areas) were estimated for each of the three Lorentzian bands in a nitroxide spectrum [$(\pi/\sqrt{3})hw^2$], where h is the peak-to-peak height and w the peak width. For a typical 3-peak nitroxide spectrum, the total spectral intensity (relative units) is then obtained by adding the three areas of the low, center, and high field peaks.

3 Results

3.1 Characterization of CaM and SL-CaM

Bovine brain CaM was purified to homogeneity, and several physicochemical characteristics are given in the Supplement. As also documented in the Supplement, SL-CaM was modified, on the average, at 2.7 methionyl residues, with no evidence of histidine, α-amino groups, or other modifications. The chemical analysis required separation and quantitation of SL-CaM acid-hydrolyzates, with recoveries assumed to be 100%. This is unlikely, but at this time we cannot distinguish homogeneity in labeling, e.g. three methionines modified, or heterogeneity in the sample, e.g. some molecules doubly labeled and others triply labeled. Importantly, a variety of physicochemical characteristics were the same or nearly so for CaM and SL-CaM (see Supplement). Thus, in this paper we will consider that 2-3 methionines are nitroxide-labeled at the thioether side chains [52, 53].

3.2 PDE Activation by CaM and SL-CaM

As shown earlier, SL-CaM activates phosphodiesterase with essentially the same V_{max}, but higher protein concentrations are required [33]. We have determined that the apparent K_d for the CaM or SL-CaM-PDE interaction is 4.8 nM and 40 nM, respectively, at a saturating concentration of Ca^{2+}, with respective V_{max}s of 3.75 and 4.28. Normalizing the V_{max} to 1.0 for CaM and SL-CaM and plotting the fractional change in enzyme velocity, $(V\text{-}V_o)/(V_{max}\text{-}V_o)$, where V_o is the basal activity, vs. $-\log_{10} (Ca^{2+})_f$, shows that the Ca^{2+} dependence for PDE activation is the same for CaM and SL-CaM (Fig. 1). The $p(Ca^{2+})_f$ values

corresponding to the half-maximal stimulation of enzymic activity are 6.84 and 6.73 for CaM and SL-CaM, respectively, a difference probably within experimental error.

3.3 CD Spectroscopy of CaM and SL-CaM

Far ultraviolet CD spectra of CaM and SL-CaM, ± Ca^{2+} and in the presence of 7 M guanidinium chloride, are shown in Supplement Fig. 1. The spectra reflect the n-π* (222 nm) and low energy component of the π-π* (208.5 nm) transitions of the proteins, and the secondary structure, primarily α-helix, appears less in SL-CaM than in CaM. However, CD spectroscopy may not be a highly reliable method for determining secondary structures in proteins [54]. With SL-CaM, in particular, the nitroxide moiety is a chromophore in the far ultraviolet, and its contribution to CD is unknown. Our interest in CD is to use the Ca^{2+}-dependent changes in mean residue ellipticity to compare CaM and SL-CaM. Fig. 2 shows the forward and reverse Ca^{2+} titrations for CaM and SL-CaM. The Ca^{2+} dependence is essentially identical in the native and spin labeled protein, e.g. the $p(Ca^{2+})_f$ corresponding to a 50% change in ellipticity is 6.68 for CaM and 6.76 for SL-CaM in the forward titrations, i.e. going from low to high Ca^{2+}. The reverse titration, from high to low Ca^{2+} concentrations, are also similar for CaM and SL-CaM, but the $p(Ca^{2+})_f$ values are somewhat higher, e.g. 7.12 and 7.35. This difference is attributed to the higher ionic strength associated with the reverse titrations.

3.4 EPR Spectroscopy of SL-CaM

The g-factor and hyperfine splitting constant A were found to be invariant to Ca^{2+} concentration between 0 - 8.1 mM Ca^{2+} for free spin label and SL-CaM, although the protein-associated label was different from that of the free label (Table 1). The difference, albeit small, is significant, and in this study it is the difference that is important since an absolute calibration of the instrument is required for an exact determination of the g-factor. The small increase in g and decrease in A indicate that the spin labels are in a less polar environment when attached to proteins, as expected.

EPR spectra are shown in Fig. 3 for SL-CaM; in contrast to this Ca^{2+}-dependent spectral change for SL-protein, the EPR spectrum from a 40 Gauss scan of 10 mM free spin label in 50 mM Tris-HCl, pH 7.5, containing either 1.0 mM Ca^{2+} or 10 mM EGTA, was identical (data not shown). Since the addition of Ca^{2+} to apo-SL-CaM, but not free spin label, resulted in a significant spectral collapse, it was important to insure that the observed spectral change represented an intramolecular event, and not an intermolecular interaction. For this, the apparent spectral intensity, determined as the sum of the areas under the three resolved peaks, was measured as a function of SL-CaM concentration in the presence and absence of Ca^{2+} (Supplement Fig. 2). The results are linear up to at least 1 mM Ca^{2+}, thus eliminating intermolecular spin-spin interactions and dipole-dipole coupling as contributory to the spectral change.

Another important check on the validity of the spectra was to determine that the responses were linear with the square root of the power used for solution measurements (5 mW). Hence a power saturation experiment was performed in the presence and absence of Ca^{2+}. As shown in Supplement Fig. 3, the low field peak height increased linearly with the square

root of power up to some 15 mW; at higher power, nonlinearity was observed. These results demonstrate that at 5 mW we are well within the linear range. Upon normalizing each set of data to the maximum peak height at 150 mW, the results for apo-SL-CaM and Ca^{2+}-saturated SL-CaM become superimposable. Thus, one can infer that the apparent spin-lattice relaxation time, T_1, of SL-CaM is not altered when Ca^{2+} binds to SL-CaM, since the reciprocal of T_1 is proportional to the slope of the curve.

Confident that we were monitoring intramolecular events and operating in a linear response region, we proceeded to analyze the EPR spectra over a wide range of Ca^{2+} concentrations. The spectral intensity (sum of the areas of the three Lorentzian bands shown in Fig. 3) was determined as a function of free Ca^{2+} concentration, and the data are presented in Fig. 4. These results indicate a Ca^{2+}-dependent transition occurring at a $p(Ca^{2+})_f$ of 6.4, a value corresponding to a higher Ca^{2+} concentration than found with either enzymic activation or CD spectroscopy.

In an effort to dissect the EPR spectra in greater depth, analyses were made of peak heights at the different Ca^{2+} concentrations. The peak heights for the low, center, and high field peaks are presented in Fig. 5. Each of the three peaks exhibited an apparent transition with increasing concentration of Ca^{2+}. Of interest, however, is that the Ca^{2+} transition midpoint (6.36 for the low and high field peaks and 6.39 for the center field peak) is again higher than that found with phosphodiesterase activity and CD measurements under the same conditions. As expected, there was no effect of Ca^{2+} on the peak heights of the free spin label (data not shown). A plot of peak height ratios, i.e. the low and high field peaks to the center field peak, indicated two possible transitions, albeit rather subtle changes, at free $p(Ca^{2+})$s of 6.49 and 6.19 when monitored by (h_{+1}/h_o), but not with (h_{-1}/h_o) (Supplement Fig. 4). Again as expected, the peak height ratios of free spin label were independent of Ca^{2+} concentration. In contrast to the transitions indicated by peak heights and as shown in Supplement Fig. 5, the widths of the low and center field peaks decrease very slightly with increasing Ca^{2+} concentration with no indication of a transition, while that of the high field peak exhibits a change in slope at a $p(Ca^{2+})_f$ of about 7 and then decreases in a linear manner to a $p(Ca^{2+})_f$ of nearly 3. Over the broad range of Ca^{2+} concentrations explored, peak widths of the free spin label were constant, about 1.30 - 1.35 Gauss.

The EPR spectra of SL-CaM precipitated with $(NH_4)_2SO_4$ (± Ca^{2+}) are shown in Supplement Fig. 6, and it can be seen that the low and high field peaks are broader in the presence of Ca^{2+}. The probable heterogeneity of the sample precludes any quantitative interpretation of these results, but the spectral differences ± Ca^{2+} again argue for a Ca^{2+}-mediated conformational change even under these conditions.

4 Discussion

Using a combination of CaM-mediated cyclic nucleotide phosphodiesterase activation of native and SL-CaM, CD spectroscopy of native and SL-CaM, and EPR spectroscopy of nitroxide-modified methionines on SL-CaM, this work has shown that the $p(Ca^{2+})_f$ values for the transition midpoints obtained by EPR occur at a higher Ca^{2+} concentration than those observed with enzyme activation and CD. For example, several EPR spectral parameters,

including spectral intensity, the three peak heights, and the (h_{+1}/h_0) peak ratio yield a mean ± SD = 6.40 ± 0.05 (n = 5). A comparison of this value to the mean ± SD of the transition midpoints obtained for CaM and SL-CaM from CD {$[\Theta]_{222\ nm}$} and phosphodiesterase activation, 6.75 ± 0.07 (n = 4), shows a significant difference, $P < 0.0001$, strongly suggesting that EPR is monitoring a distinct conformational transition. Since the Ca^{2+}-mediated transition midpoints for native CaM are the same as those for SL-CaM when determined by enzyme activation and CD, one has confidence that the midpoints from EPR measurements of SL-CaM reflect an intrinsic property of the protein, not one introduced by the covalently attached nitroxides. It is likely that the Ca^{2+}-dependent transition determined by EPR spectroscopy corresponds to the binding of Ca^{2+} to the N-terminal sites. The sensitivity of this technique to the putative binding of the last two Ca^{2+}s offers another probe to explore CaM interactions with target proteins. Similar to our interpretation of the EPR results of SL-CaM, data from hydrogen-deuterium exchange and Fourier transform infrared spectroscopy were interpreted to indicate binding to the third and fourth Ca^{2+} sites [20].

Others have used the spin-labeling reagent described herein [34-36, 39, 40], a few with slight modifications to the conditions originally given [33], and, in some cases, reported different results. For example, standardizing with free spin label and native CaM, and then using the absorption at 257 nm as a measure of incorporated spin label, one study reported just one spin label per molecule of CaM [36]. Although spectral intensities were not shown in this report, the peak height ratio, (h_{-1}/h_0), was found to decrease with increasing Ca^{2+} through the transition, as also observed by others [40]. These apparent discrepancies can perhaps be reconciled to some extent by the experimental conditions used and possible stoichiometric differences in the number of protein-incorporated spin labels; in the present case, however, there is confidence that at least two, and most likely three, spin labels are attached per CaM.

The multiple labeling of methionines presents both advantages and disadvantages. The advantage is that, due to Ca^{2+}-dependent conformational changes in the protein that alter the relative proximity and microenvironments of the nitroxides, dramatic changes in the EPR spectra of SL-CaM accompany Ca^{2+} binding. The obvious disadvantage is that the spectra cannot be dissected and interpreted fully in a quantitative manner, particularly when the sites of labeling are unknown. In particular, the rotation correlation time, τ_c, is a useful parameter accessible by EPR; however, the presence of multiple methionine labeling precludes such an estimate for SL-CaM.

In EPR spectroscopy the spin Hamiltonian is composed of four terms as illustrated below. The first two terms account for the 3-line spectrum of nitroxides, and the latter two terms become important when more than one spin probe is utilized, e.g. on the same protein or on two interacting proteins, or when a spin probe comes in close proximity to another paramagnetic species, e.g. certain metals.

$$H = H_{ZI} + H_{NHI} + H_{DDI} + H_{SSEI}$$

In this equation H_{ZI} refers to the Zeeman interaction arising from the interaction between the unpaired electron spin and the external magnetic field, H_{NHI} denotes the nuclear hyperfine interaction resulting from the association of the unpaired electron with the ^{14}N nucleus, H_{DDI} accounts for dipole-dipole coupling (sensitive at distances ≥ 10Å), $H_{SSEI}$and pertains to the spin exchange interaction (manifested at distances □ 10Å). All terms are possibly important in the present study due to the multiple spin labeling of a single protein. Moreover, the different spin labels are likely to be in distinct microenvironments, and, thus, the spectra probably reflect a composite of two, or more likely three, nitroxides, each somewhat different from the others.

From the spin Hamiltonian there is of course clear experimental evidence of the Zeeman and nuclear hyperfine interactions, and our results strongly indicate Heisenberg spin exchange and/or dipole-dipole coupling concomitant with Ca^{2+} binding to SL-CaM. For either spin exchange or dipole-dipole coupling, the expected loss of spectral intensity was observed in the EPR spectra, but there was no line broadening, which generally accompanies both spin exchange and dipole-dipole coupling. This we interpret as arising from interaction of two labels in close proximity giving sufficient broadening that is simply not observed with the solution spectra in the 100 Gauss scans at the sensitivity used. Some of the data indicate greater rotational flexibility of at least one of the probes. While these interpretations appear inconsistent, they can be reconciled if there are three spin labels attached to CaM, two of which come in close proximity upon Ca^{2+} binding, with the other one gaining rotational freedom or mobility. Peak broadening has been used most effectively to measure the distance from a spin-labeled methionine in α-lactalbumin to paramagnetic lanthanide bound to the high-affinity Ca^{2+} binding site on the protein [56]. Also, Heisenberg spin exchange and dipolar broadening provide considerable information on doubly labeled proteins [57-61].

It is prudent to briefly review pertinent studies in the literature dealing with reactivities and environments of the methionyl side chains in CaM. Early studies using oxidation to convert Met to methionine sulfoxide with N-chlorosuccinimide reported the modification of 3-4 methionines when CaM was labeled in the presence of Ca^{2+} at neutral or slightly alkaline pH [62]. Additional analyses led to the suggestion that residues 71, 72, and 76 in the central helix were so modified, and possibly 109 as well [63]. More recently, using a nitroxide spin label and 2-dimensional NMR to map the line widths and relaxation rates of the individual methionine residues, it was found that the methionines are almost completely buried in apo-CaM and become almost fully exposed when the protein is saturated with Ca^{2+} [64]. It was also reported that the binding of three peptides from target proteins reduces accessibility of the nitroxide probe to most of the methionines; however, different modes of binding were observed. Another report using hydrogen peroxide to oxidize Met side chains concluded that one of the vicinal methionines, Met^{144} or Met^{145}, was selectively oxidized [65]. On the other hand, selective oxidation of CaM methionyl groups with methionine sulfoxide reductase A showed that, in the presence of Ca^{2+}, Met^{76} was modified [66].

Others have used two-dimensional [^{1}H,^{13}C]-heteronuclear multiple quantum coherence (HMQC) NMR spectroscopy of (*methyl*-^{13}C)-labeled methionyl groups to monitor the environment and T_1 relaxation rates of the methionines in CaM [67]. They found that each

of the nine methionyl side chains is located within a slightly different microenvironment and that the relaxation rates are longer in the Ca^{2+}-occupied state than in the Ca^{2+}-free form, consistent with the high degree of solvent exposure. In a follow-up study, again using HMQC NMR spectroscopy of ^{13}C-labeled methionines and a free, i.e. unattached, spin label to monitor solvent exposure of methionyl side chains, the surprising observation was made that Met^{76}, unlike the other Met methyl groups, was not fully exposed. These reports suggest solvent exposure of all the methionyl side chains of Ca^{2+}-CaM and further indicate that those Mets in the central helix and perhaps those near the C-terminus are most likely the ones to be modified by the spin labeling reagent used herein.

It is helpful to review the structures of apo-CaM and $(Ca^{2+})_4$-CaM when discussing Met labeling, and Fig. 6 shows results from NMR spectroscopy and crystallography with the nine methionyl residues highlighted (taken from structures deposited in the Protein Data Bank [12]). Knowing the relative positions of the methionyl residues from the structures of apo-CaM and $(Ca^{2+})_4$-CaM, it is tempting to make plausible estimates of the residues that could be spin labeled using the EPR results to guide assignments, albeit tentative. (A structure of $(Ca^{2+})_2$-CaM is available [68], but this form is in complex with anthrax adenylyl cyclase and thus not suitable for the comparison being done.) Consistent with the EPR results and assuming that if two Met side chains in apo-CaM approach within 9 Å of each other concomitant with Ca^{2+} binding and interact, either via Heisenberg spin exchange and/or dipole-dipole coupling, then the number of possibilities from the 36 combinations are limited. (The value of 9 Å was chosen since spin exchange interactions are usually dominant at distances □ 10 Å.)

As measured between sulfur atoms, several methionine side chains are in close proximity in both apo-CaM and $(Ca^{2+})_4$-CaM; others are relatively close in apo-CaM but become separated upon Ca^{2+} binding; and most of the pairwise separations are too far apart in both forms of CaM to interact productively and alter the EPR spectrum. The major contenders for interacting pairs are residues 36 – 51, 71 – 72, 71 – 76, 72 – 76, 144 – 145, and possibly 109 – 124, although the estimated difference in distance ± Ca^{2+} between 109 – 124 is just 0.7 Å. These results, consistent with earlier reports [62, 63, 65], suggest that spin labels could be located on methionine residues in the central helix (residues 71, 72, and/or 76), as well as the C-terminal domain (residues 109, 144, and/or 145). There is no evidence in the literature regarding reactivities of residues 36 and 51, but it is of course possible that one or both of these Mets may be spin labeled. In view of our interpretation that the EPR spectral changes arise from Ca^{2+} binding to the N-terminal sites and the report of a compact to more extended form of CaM in going from the $(Ca^{2+})_2$-form to the $(Ca^{2+})_4$-form [69, see below], likely candidates for modification would be the methionines in the central helix and perhaps the N-terminal lobe. It should also be mentioned that the size of the spin labeling reagent is a factor, as it is some 4 -5 Å in length. It is expected that the attached spin labels will have some rotational freedom, and, if so, they could be closely packed.

Of related interest to the findings reported herein is the observation, based on studies using time-resolved small angle X-ray scattering along with flash photolysis of caged Ca^{2+}, that, upon binding two Ca^{2+} ions to the C-terminal domain, CaM adopts a compact structure distinct from that when the last two Ca^{2+} sites are filled and mastoparan is bound [69]. In the

absence of mastoparan, Ca^{2+} binding to the N-terminal domain leads to the extended form found with X-ray crystallography. Thus, that work establishes a 3-state model for CaM as it progresses from the Ca^{2+}-free state to the $(Ca^{2+})_4$-form in the absence of regulatory protein or peptide (see below), with each form having a different conformation. Supporting this observation is the report of a closed compact structure of CaM when crystallized at pH 5.6 [10]. We posit that the Ca^{2+}-mediated EPR changes of SL-CaM discussed herein are detecting the $[(Ca^{2+})_2\text{-CaM}] \rightarrow [(Ca^{2+})_4\text{-CaM}]$ transition, i.e. the filling of the two N-terminal sites.

$$CaM + 2Ca^{2+} \leftrightarrow \left[\left(Ca^{2+}\right)_2 - CaM\right] + 2Ca^{2+} \leftrightarrow \left[\left(Ca^{2+}\right)_4 - CaM\right]$$

In summary, this work has shown that calmodulin can be modified with nitroxide spin labels at methionyl residues (probably three) and that the Ca^{2+}-mediated changes in spectral intensity are consistent with Heisenberg spin exchange and/or dipole-dipole coupling. The spin-labeled protein exhibits identical responses to Ca^{2+} as native protein when monitored by CD spectroscopy and PDE activation. In contrast, the midpoint of the Ca^{2+}-dependent changes in spectral intensity and peak heights occurs at a higher Ca^{2+} concentration than observed with CD and enzyme activation, suggesting that the spin probes are sensitive to the filling of the N-terminal binding sites and thus detecting the transition from the compact form, $[(Ca^{2+})_2\text{-CaM}]$, to the more extended form, $[(Ca^{2+})_4\text{-CaM}]$. Thus, this method offers a different approach for studying Ca^{2+}-mediated conformational changes of CaM and may prove useful for monitoring interactions with target proteins.

Supplementary Material

Refer to Web version on PubMed Central for supplementary material.

Acknowledgments

We are most appreciative of the helpful comments, suggestions, and assistance from Professors Malcolm Forbes (University of North Carolina), William Lanzilotta (University of Georgia), John Rose (University of Georgia), Alex Smirnov (North Carolina State University), and Zachary Wood (University of Georgia). We also thank Professor Albert Beth (Vanderbilt University) for helpful discussions and for obtaining EPR spectra of precipitated spin-labeled calmodulin. Lastly, a special thanks to Mr. Edward Larry Bowman for his invaluable assistance in preparing the figures and to Mr. Connor Puett for his expert help. This research was supported by the National Institutes of Health (Grants DK33973, GM35415, GM07319, and RR05424).

Abbreviations

CaM	calmodulin
CD	circular dichroism
EGTA	ethylene glycol-*bis*(2-aminoethylether-*N*,*N*,*N*,*N*-tetraacetic acid
EPR	electron paramagnetic resonance
HMQC	heteronuclear multiple quantum coherence
mW	milliwatts

NMR	nuclear magnetic resonance
PDE	phosphodiesterase (cyclic nucleotide)
SEM	standard error of the mean
SL-CaM	spin-labeled calmodulin

References

1. Chin D, Means AR. Calmodulin: A prototypical sensor. Trends Cell Biol. 2000; 10:322–328. [PubMed: 10884684]
2. Means AR. The year in basic science: Calmodulin kinase cascades. Mol Endocrinol. 2008; 22:2759–2765. [PubMed: 18845671]
3. Babu YS, Sack JS, Greenhough TJ, Bugg CE, Means AR, Cook WJ. Three-dimensional structure of calmodulin. Nature. 1985; 315:37–40. [PubMed: 3990807]
4. Babu YS, Bugg CE, Cook WJ. Structure of calmodulin refined at 2.2 Å resolution. J Mol Biol. 1988; 204:191–204. [PubMed: 3145979]
5. Chattopadhyaya R, Meador WE, Means AR, Quiocho FA. Calmodulin structure refined at 1.7 Å resolution. J Mol Biol. 1992; 228:1177–1192. [PubMed: 1474585]
6. Kuboniwa H, Tjandra N, Grzesiek S, Ren H, Klee CB, Bax A. Solution structure of calcium-free calmodulin. Nat Struct Biol. 1995; 2:768–776. [PubMed: 7552748]
7. Finn BE, Evenas J, Drakenberg T, Waltho JP, Thulin E, Forsen S. Calcium-induced structural changes and domain autonomy in calmodulin. Nature Struct Biol. 1995; 2:777–783. [PubMed: 7552749]
8. Wilson MA, Brunger AT. The 1.0 Å crystal structure of Ca^{2+}-bound calmodulin: An analysis of disorder and implications for functionally relevant plasticity. J Mol Biol. 2000; 301:1237–1256. [PubMed: 10966818]
9. Chou JJ, Li S, Klee CB, Bax A. Solution structure of Ca^{2+}-calmodulin reveals flexible hand-like properties of its domains. Nat Struct Biol. 2001; 8:990–996. [PubMed: 11685248]
10. Fallon JL, Quiocho FA. A closed compact structure of native Ca^{2+-} calmodulin. Structure. 2003; 11:1303–1307. [PubMed: 14527397]
11. Kumar V, Chichili VPR, Tang X, Sivaraman J. A novel trans conformation of ligand-free calmodulin. PLoS ONE. 2013; 8:e54834. [PubMed: 23382982]
12. Protein Data Bank. 2013. [http://www.rcsb.org/pdb/]
13. Yap KL, Kim J, Truong K, Sherman M, Yuan T, Ikura M. Calmodulin target database. J Struct Funct Genomics. 2000; 1:8–14. [http://calcium.uhnres.utoronto.ca/ctdb/]. [PubMed: 12836676]
14. Wall ME, Clarage JB, Phillips GN Jr. Motions of calmodulin characterized using both Bragg and diffuse X-ray scattering. Structure. 1997; 5:1599–1612. [PubMed: 9438860]
15. Meador WE, Means AR, Quiocho FA. Modulation of calmodulin plasticity in molecular recognition on the basis of X-ray structures. Science. 1993; 262:1718–1721. [PubMed: 8259515]
16. Tidow H, Nissen P. Structural diversity of calmodulin binding to its target sites. FEBS J. 2013:1–15.
17. Crouch TH, Klee CB. Positive cooperative binding of calcium to bovine brain calmodulin. Biochemistry. 1980; 19:3692–3698. [PubMed: 7407067]
18. Masino L, Martin SR, Bayley PM. Ligand binding and thermodynamic stability of a multidomain protein, calmodulin. Prot Sci. 2000; 9:1519–1529.
19. VanScyoc WS, Shea MA. Phenylalanine fluorescence studies of calcium binding to N-domain fragments of Paramecium calmodulin mutants show increased calcium affinity correlates with enhanced disorder. Prot Sci. 2001; 10:1758–1768.
20. Yu T, Wu G, Yang H, Wang J, Yu S. Calcium-dependent conformational transition of calmodulin determined by Fourier transform infrared spectroscopy. Int J Biol Macromol. 2013; 56:57–61. [PubMed: 23403030]

21. Hellstrand E, Kukora S, Shuman CF, Steenbergen S, Thulin E, Kohli A, Krouse B, Linse S, Åkerfeldt KS. Förster resonance energy transfer studies of calmodulin produced by native protein ligation reveal inter-domain electrostatic repulsion. FEBS J. 2013; 280:2675–2687. [PubMed: 23552119]
22. Sorensen BR, Shea MA. Calcium binding decreases the Stokes radius of calmodulin and mutants R74A, R90A, and R90G. Biophys J. 1996; 71:3407–3420. [PubMed: 8968610]
23. Berliner, LJ. Spin labeling: Theory and applications. Academic Press; New York, New York: 1976.
24. Berliner, LJ. Spin labeling II: Theory and applications. Academic Press; New York, New York: 1979.
25. Berliner, LJ.; Reuben, J. Biological magnetic resonance. Vol. 8. Plenum Press; New York, New York: 1989. Spin labeling: Theory and applications..
26. Fajer, PG. Electron spin resonance spectroscopy labeling in peptide and protein analysis.. In: Meyers, RA., editor. Encycl Anal Chem. John Wiley & Sons Ltd; Chichester, UK: 2000. p. 5725-5761.
27. Bender, CJ.; Berliner, LJ. Computational and instrumental methods in EPR. Biological magnetic resonance 25. Springer Science; New York, New York: 2006.
28. Fanucci GE, Cafiso DS. Recent advances and applications of site-directed spin labeling. Curr Opin Struct Biol. 2006; 16:644–653. [PubMed: 16949813]
29. White GF, Ottignon L, Georgiou T, Kleanthous C, Moore GR, Thomson AJ, Oganesyan VS. Analysis of spin label motion in a protein-protein complex using multiple frequency EPR spectroscopy. J Mag Res. 2007; 185:191–203.
30. Klare JP, Steinhoff H-J. Spin Labeling EPR. Photosynth Res. 2009; 102:377–390. [PubMed: 19728138]
31. Drescher M. EPR in protein science: Intrinsically disordered proteins. Top Curr Chem. 2012; 321:91–120. [PubMed: 21826602]
32. Hubbell WL, Lopez CJ, Altenbach C, Yang Z. Technological advances in site-directed spin labeling of proteins. Curr Opin Struc Biol. 2013; 23:1–9.
33. Hewgley PB, Puett D. Spin labeled calmodulin: A new probe for studying Ca^{2+} and macromolecular interactions. Ann NY Acad Sci. 1980; 356:20–32. [PubMed: 6263148]
34. Giedroc DP, Ling N, Puett D. Identification of β-endorphin residues 14-25 as a region involved in the inhibition of calmodulin-stimulated phosphodiesterase activity. Biochemistry. 1983; 22:5584–5591. [PubMed: 6317022]
35. Siegel N, Coughlin R, Haug A. A thermodynamic and electron paramagnetic resonance study of structural changes in calmodulin induced by aluminum binding. Biochem Biophys Res Commun. 1983; 115:512–517. [PubMed: 6312983]
36. Xu YH, Gietzen K, Galla H-J. Electron paramagnetic resonance study of calmodulin: Conformational change and interaction with divalent cations. Int J Biol Macromol. 1983; 5:154–158.
37. Jackson AE, Puett D. Specific acylation of calmodulin: Synthesis and adduct formation with a fluorenyl-based spin label. J Biol Chem. 1984; 259:14985–14992. [PubMed: 6094585]
38. Nieves J, Kim L, Puett D, Echegoyen L, Benabe J, Martinez-Maldonado M. Electron spin resonance of calmodulin-vanadyl complexes. Biochemistry. 1987; 26:4523–4527. [PubMed: 2822096]
39. Buccigross JM, Nelson DJ. Interactions of spin-labeled calmodulin with trifluoperazine and phosphodiesterase in the presence of Ca(II), Cd(II), La(III), Tb(III), and Lu(III). J Inorg Biochem. 1988; 33:139–147. [PubMed: 2842452]
40. You G, Nelson DJ. Al^{3+} versus Ca^{2+} ion binding to methionine and tyrosine spin-labeled bovine brain calmodulin. J Inorg Biochem. 1991; 41:283–291. [PubMed: 1647442]
41. Yacko MA, Vanaman TC, Butterfield DA. Spin labeling studies of wheat germ calmodulin in solution. Biochim Biophys Acta. 1991; 1064:7–12. [PubMed: 1851042]
42. Yacko MA, Butterfield DA. Spin-labeling studies of the conformation of the Ca^{2+}regulatory protein calmodulin in solution and bound to the membrane skeleton in erythrocyte ghosts: Implications to transmembrane signaling. Biophys J. 1992; 63:317–322. [PubMed: 1330029]

43. Zhou YA, Li Y, Wang ZG, Ou YH, Zhou X. ^{1}H NMR and spin-labeled EPR studies on the interaction of calmodulin with jujuboside A. Biochem Biophys Res Commun. 1994; 202:148–154. [PubMed: 8037706]
44. Qin Z, Squier TC. Calcium-dependent stabilization of the central sequence between Met^{76} and Ser^{81} in vertebrate calmodulin. Biophys J. 2001; 81:2908–2918. [PubMed: 11606301]
45. Shao J, Cieslak J, Gross A. Generation of a calmodulin-based EPR calcium indicator. Biochemistry. 2009; 48:639–644. [PubMed: 19115960]
46. Qin Z, Wertz SL, Jacob J, Savini Y, Cafiso DS. Defining protein-protein interactions using site-directed spin-labeling: The binding of protein kinase C substrates to calmodulin. Biochemistry. 1996; 35:13272–13276. [PubMed: 8873591]
47. Tombolato F, Ferrarini A, Freed JH. Modeling the effects of structure and dynamics of the nitroxide side chain on the ESR spectra of spin-labeled proteins. J Phys Chem. 2006; 110:26260–26271.
48. Likhtenshtein, GI.; Yamauchi, J.; Nakatsuji, S.; Smirnov, AI.; Tamura, R., editors. Nitroxides: Applications in Chemistry, Biomedicine, and Materials Science. Wiley-VCH Verlag GmbH & Co.; KGaA, Weinheim, Germany: 2008.
49. Nesmelov YE, Thomas DD. Protein structural dynamics revealed by site-directed labeling and multifrequency EPR. Biophys Rev. 2010; 2:91–99. [PubMed: 21687819]
50. Jeschke G. Conformational dynamics and distribution of nitroxide spin labels. Prog Nuc Mag Res Spect. 2013; 72:42–60.
51. Rybalkin, SD.; Hinds, TR.; Beavo, JA. Enzyme assays for cGMP hydrolyzing phosphodiesterases.. In: Krieg, T.; Lukowski, R., editors. Guanylate cyclase and cyclic GMP. Methods in Molecular Biology. Vol. 1020. Humana Press/Springer; 2013. p. 51-62.
52. Kosman DJ. Electron paramagnetic resonance probing of macromolecules: A comparison of structure/function relationships in chymotrypsinogen, α-chymotrypsin and anhydrochymotrypsin. J Mol Biol. 1972; 67:247–264. [PubMed: 4339191]
53. Likhtenshtein, GI. Spin Labeling Methods in Molecular Biology. Shelnitz, PS., editor. John Wiley & Sons; New York, New York: Moscow, Russia: 1976. p. 24-29.Originally published in 1974 by Isdatel stvo Nauka
54. Lin K, Yang H, Gao Z, Li F, Yu S. Overestimated accuracy of circular dichroism in determining protein secondary structure. Eur Biophys J. 2013; 42:455–461. [PubMed: 23467783]
55. O`Donnell SE, Newman RA, Witt TJ, Hultman R, Froehlig JR, Christensen AP, Shea MA. Thermodynamics and conformational change governing domain-domain interactions of calmodulin. Methods Enzymol. 2009; 466:503–526. [PubMed: 21609874]
56. Musci G, Koga K, Berliner LJ. Methionine-90-spin-labeled bovine α-lactalbumin: Electron spin resonance and NMR distance measurements. Biochemistry. 1988; 27:1260–1265. [PubMed: 2835087]
57. Rabenstein MD, Shin Y-K. Determination of the distance between two spin labels attached to a macromolecule. Proc Natl Acad Sci. 1995; 92:8239–8243. [PubMed: 7667275]
58. Mchaourab HS, Oh KJ, Fang CJ, Hubbell WL. Conformation of T4 lysozyme in solution: Hinge-bending motion and the substrate-induced conformational transition studied by site-directed spin labeling. Biochemistry. 1997; 36:307–316. [PubMed: 9003182]
59. Berliner, LJ.; Eaton, SS.; Eaton, GR., editors. Biological Magnetic Resonance. Vol. 19. Kluwer Acedemic/Plenum Publishing; New York. New York: 2000. Distance measurements in biological systems by EPR..
60. Pyka J, Ilnicki J, Altenbach C, Hubbell WL, Froncisz W. Accessibility and dynamics of nitroxide side chains in T4 lysozyme measured by saturation recovery EPR. Biophys J. 2005; 89:2059–2068. [PubMed: 15994892]
61. Altenbach C, Froncisz W, Hemker R, Mchaourab H, Hubbell WL. Accessibility of nitroxide side chains: Absolute Heisenberg exchange rates from power saturation EPR. Biophys J. 2005; 89:2103–2112. [PubMed: 15994891]
62. Walsh M, Stevens FC. Chemical modification studies on the Ca^{2+} ion- dependent protein modulator of cyclic nucleotide phosphodiesterase. Biochemistry. 1977; 16:2742–2749. [PubMed: 196618]

63. Walsh M, Stevens FC. Chemical modification studies on the Ca^{2+}-dependent protein modulator: The role of methionine residues in the activation of cyclic nucleotide phosphodiesterase. Biochemistry. 1978; 17:3924–3930. [PubMed: 213097]

64. Yuan T, Ouyang H, Vogel HJ. Surface exposure of the methionine side chains of calmodulin in solution. J Biol Chem. 1999; 274:8411–8420. [PubMed: 10085072]

65. Yao Y, Yin D, Jas GS, Kuczera K, Williams TD, Schoneich C, Squier TC. Oxidative modification of a carboxyl-terminal vicinal methionine in calmodulin by hydrogen peroxide inhibits calmodulin-dependent activation of the plasma membrane Ca-ATPase. Biochemistry. 1996; 35:2767–2787. [PubMed: 8611584]

66. Lim JC, Kim G, Levine RL. Stereospecific oxidation of calmodulin by methionine sulfoxide reductase A. Free Rad Biol Med. 2013; 61:257–264. [PubMed: 23583331]

67. Siivari K, Zhang M, Palmer AG III, Vogel HJ. NMR studies of the methionine methyl groups in calmodulin. FEBS Letters. 1995; 366:104–108. [PubMed: 7789524]

68. Drum CL, Yan S-Z, Bard J, Shen Y-Q, Lu D, Soelaiman S, Grabarek Z, Bohm A, Tang W-J. Structural basis for the activation of anthrax adenylyl cyclase exotoxin by calmodulin. Nature. 2002; 415:396–492. [PubMed: 11807546]

69. Yamada Y, Matsuo T, Iwamoto H, Yagi N. A compact intermediate state of calmodulin in the process of target binding. Biochemistry. 2012; 51:3963–3970. [PubMed: 22548417]

70. Chimera. 2013. [www.cgl.ucsf.edu/chimera/]

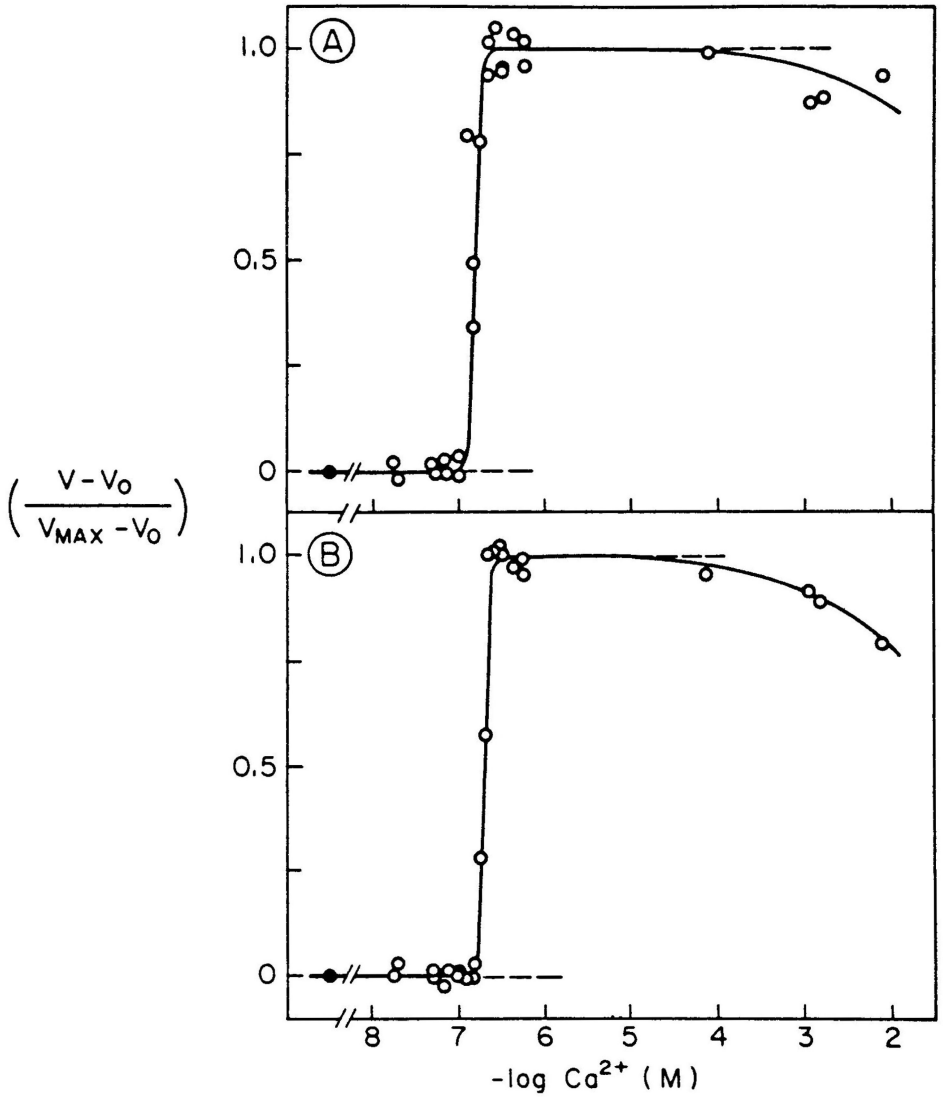

Fig. 1.

Ca^{2+}-mediated activation of phosphodiesterase by CaM and SL-CaM. CaM (A) and SL-CaM (B) were each present at a saturating concentration (3.0 μM), and the data are given in a normalized form as $(V - V_o) / (V_{max} - V_o)$, where V is the measured velocity, V_o the basal activity in the presence of 2 mM EGTA, and V_{max} the maximal activity achieved at 1 μM Ca^{2+}. The results of two independent experiments are shown, and each point denotes the mean of duplicate assays. Results in the presence of 2 mM EGTA with no added Ca^{2+} are shown as closed symbols, and the enzymic activity in the presence of 2 mM EGTA with no added Ca^{2+}, but with CaM or SL-CaM, was invariably higher than the basal activity in the absence of CaM or SL-CaM. Midpoints (pCa^{2+} for CaM and SL-CAM are 6.84 and 6.73, respectively. The abscissa is $-\log_{10} (Ca^{2+})_f$ with Ca^{2+} in units of M.

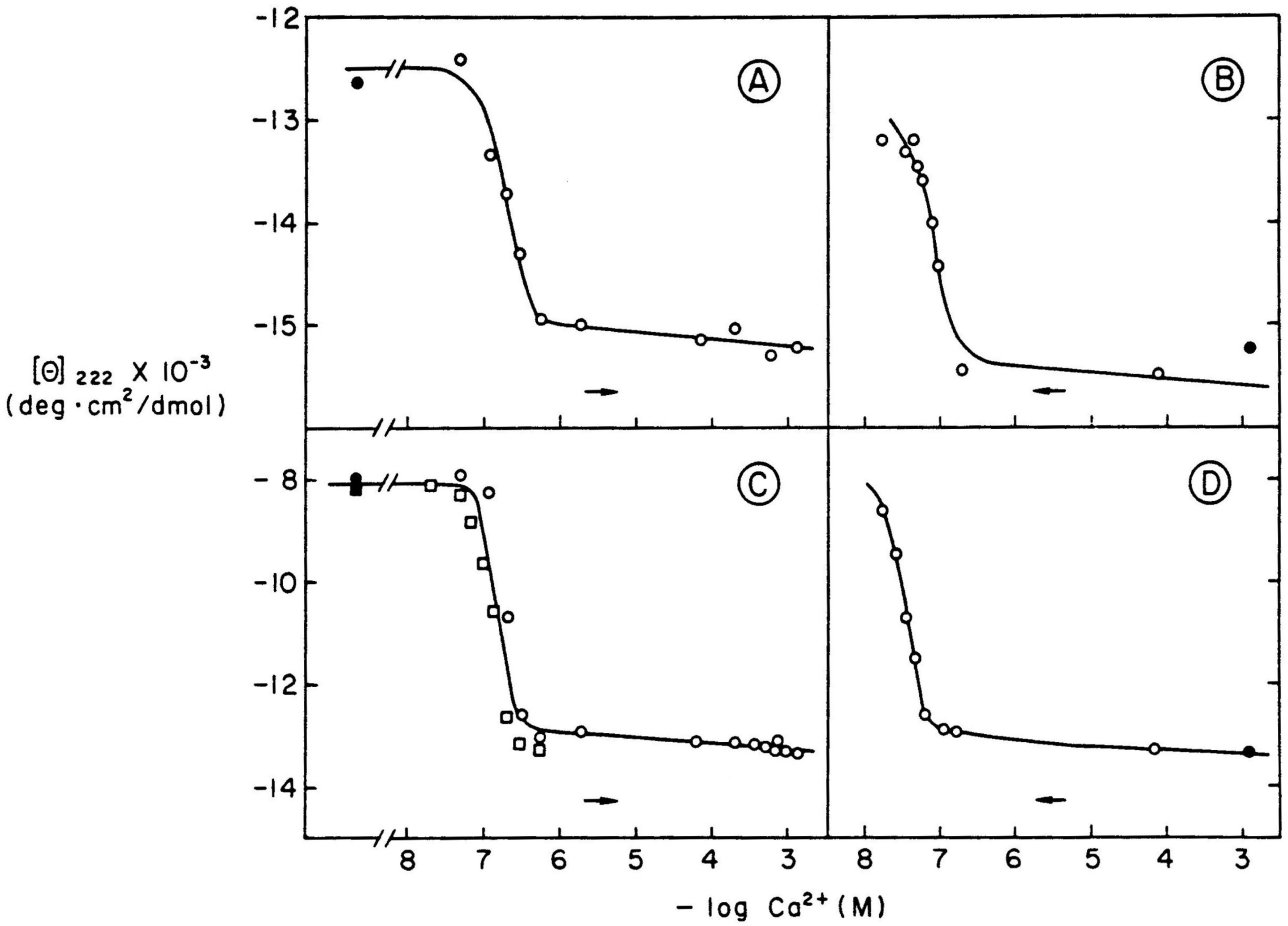

Fig. 2.

Ca $^{2+}$-induced changes in the mean residue ellipticity at 222 nm for CaM and SL-CaM. The CD changes were determined in both the forward (A, C), i.e. from 0 -1.2 mM Ca^{2+}, and reverse (B, D), i.e. from 1.2 mM Ca^{2+}, directions for CaM (A, B) and SL-CaM (C, D) in 50 mM Tris-HCl, pH 7.5 (0.26 mg/mL). The closed symbols in panels A and C denote the presence of 2 mM EGTA, and forward titrations were done with small aliquots of 0.01 M $CaCl_2$ in the same Tris-HCl buffer. The conditions were such that in going from the starting solution (0 mM Ca^{2+}) to the final solution (1.2 mM Ca^{2+}), the volume change was 4 %; appropriate corrections were made to $[\Theta]_{222\ nm}$. The closed symbols in panels B and D refer to solutions in the Tris-HCl buffer that also contained 1.93 mM EGTA and 3.55 mM $CaCl_2$; these were titrated with 0.5 mM EGTA in the Tris-HCl buffer. As above, corrections were made to the small dilution of protein. $p(Ca^{2+})_f$ midpoints of the Ca^{2+}-mediated transition are 6.68 and 6.76, respectively. The Ca^{2+} concentration is given as $-\log_{10} (Ca^{2+})_f$ with Ca^{2+} in units of M.

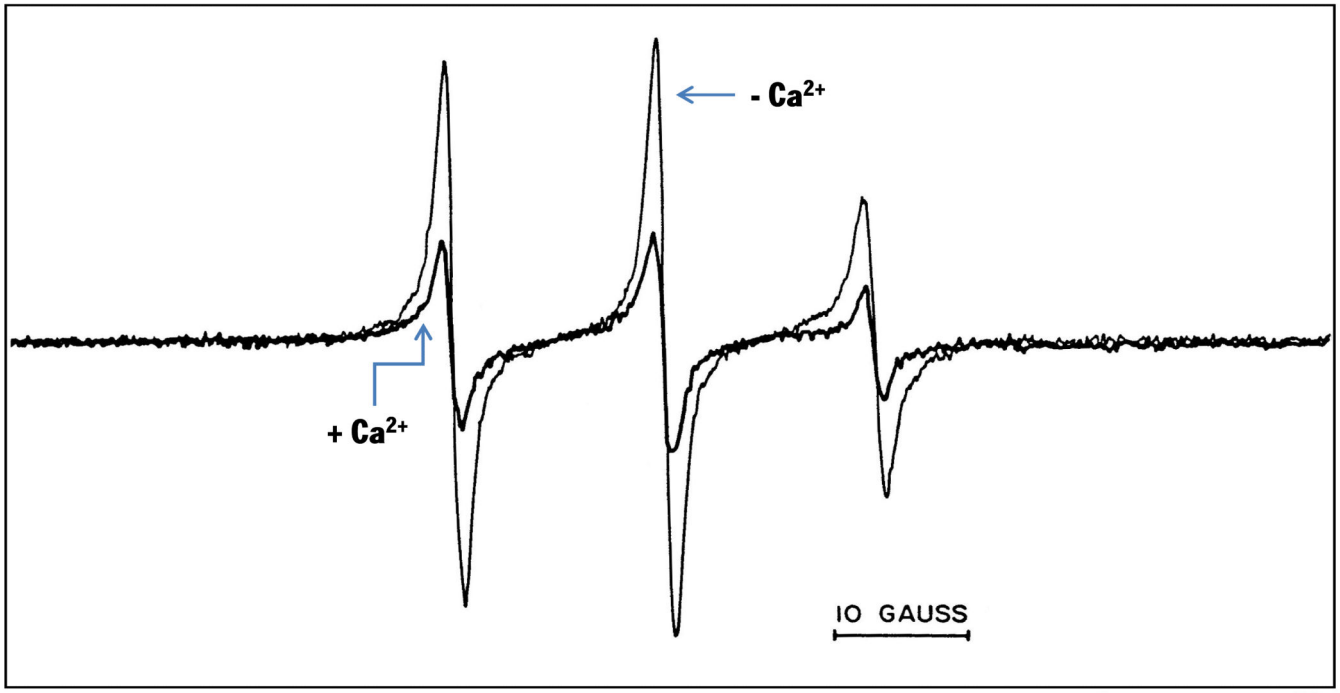

Fig. 3.

EPR spectra of SL-CaM ± Ca^{2+}. SL-CaM (29 μM) in 50 mM Tris-HCl, pH 7.5 containing 1.0 mM Ca^{2+} (heavy line and marked as +Ca^{2+}) or 10 mM EGTA (lighter line and highlighted by –Ca^{2+}). A typical 100 Gauss scan is shown.

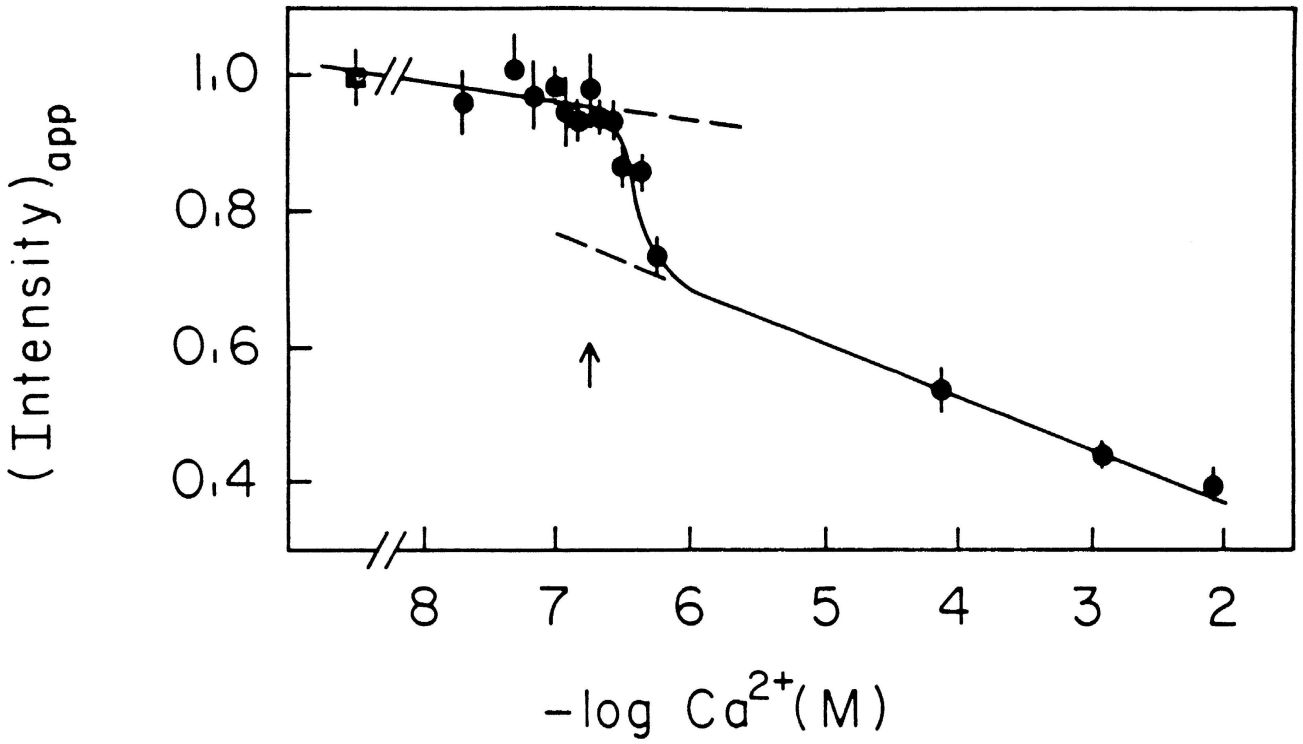

Fig. 4.

Spectral intensity of SL-CaM EPR spectra as a function of free Ca^{2+} concentration. The sum of the area of the three Lorentzian bands, obtained as described in Section 2.4, is in arbitrary units and was thus normalized to 1.0 in 2 mM EGTA (0 mM Ca^{2+}); it is designated by a square. The arrow indicates the transition midpoint observed using CD (222 nm); that for the data shown is $pCa^{2+} = 6.40$. Ca^{2+} had no effect on the intensity of the free spin label (data not shown). The abscissa is $-\log_{10} (Ca^{2+})_f$ with Ca^{2+} in units of M.

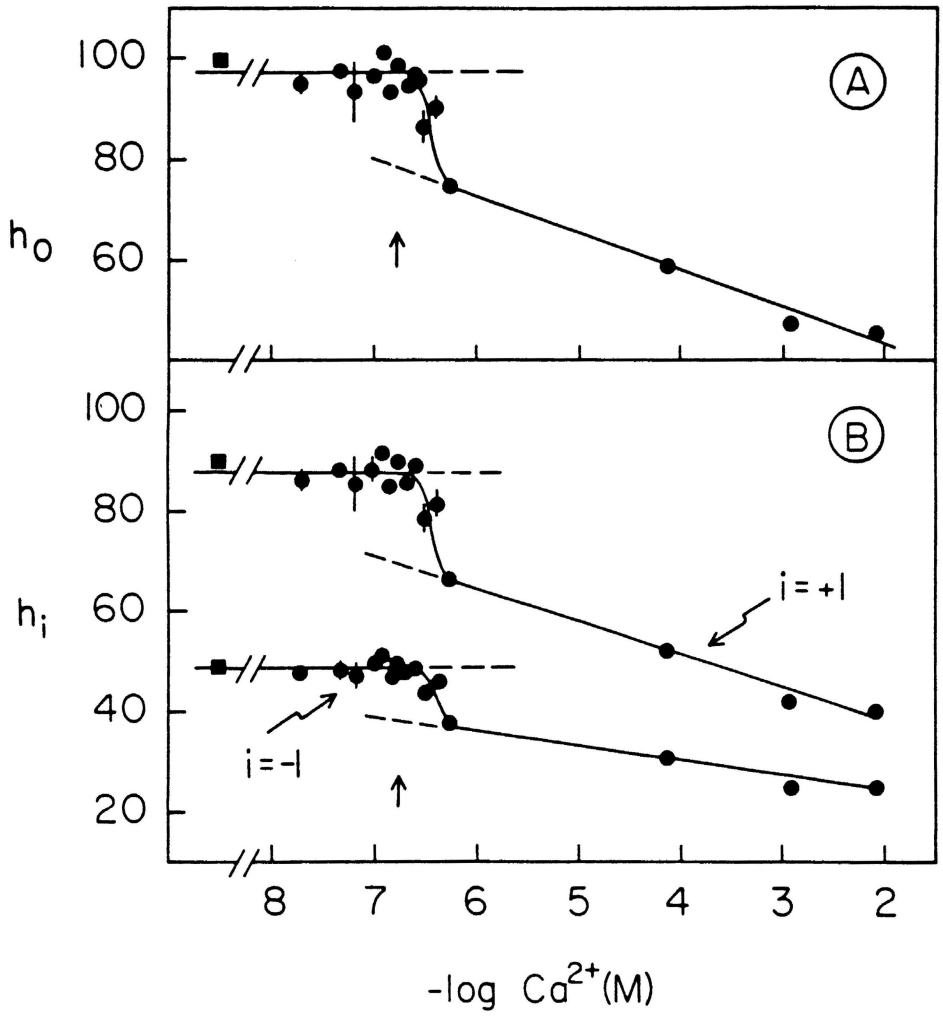

Fig. 5.

EPR resonance peak heights at various free Ca^{2+} concentrations. The peak-to peak heights in arbitrary units are shown for the center field peak (A) and the low and high field peaks (B). The transition midpoint determined at 222 nm by CD is indicated by the arrows, and the pCa^{2+} values for the peak height results are 6.36 (h_{-1}), 6.39 (h_0), and 6.36 (h_{+1}). The peak heights of the free spin label were invariant to Ca^{2+} concentration (data not shown). The Ca^{2+} concentration is shown as $-\log_{10} (Ca^{2+})_f$ with Ca^{2+} in units of M.

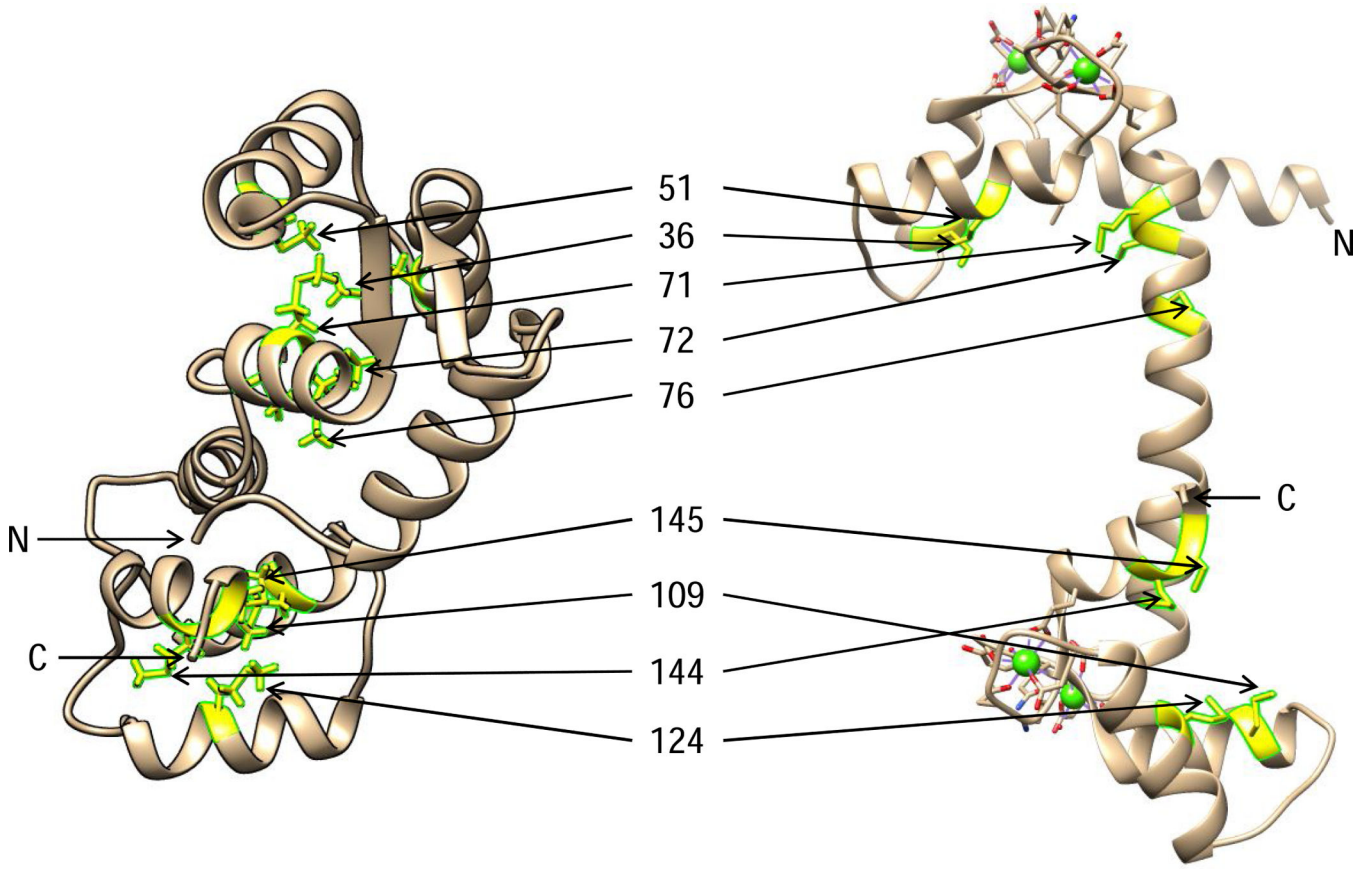

Fig. 6.

Structures of apo-CaM (left) and $(Ca^{2+})_4$-CaM (right) with the nine methionine side chains highlighted (yellow) and identified. The structures were drawn with Chimera [70], and coordinates are from the Protein Data Bank [12], referring to reports based on NMR [6] and protein crystallography [5], respectively. The two views were chosen to optimize visualization of the methionines, and the amino (N) and carboxy (C) termini are noted. The pair-wise distances between the methionines are given in Supplement Table 2 for each of the structures.

Table 1

Average g-factor and hyperfine splitting constant A of 3-(2-iodoacet-amido)-2,2,5,5-tetramethyl-1-pyrrolidinyl oxyl (free spin label) and spin-labeled calmodulin[a]

Nitroxide form	g-factor	Hyperfine splitting constant A
Free spin label (n = 17)	2.0108 ± 0.0002[b]	16.00 ± 0.01[b] Gauss
SL-CaM (n = 44)	2.0133 ± 0.0000$_4$[b]	15.92 ± 0.01[b] Gauss

[a] Measurements were made on solutions in 50 mM Tris-HCl, pH 7.5, and various EGTA:$CaCl_2$ ratios to obtain free Ca^{2+} concentrations between 0 - 8.1 mM. No effect of Ca^{2+} was noted on the free spin label (4.7 μM) or SL-CaM (0.25 – 0.26 mg/mL). The values are given as mean ± SEM.

[b] $P < 0.0001$.